Tetrahedron 66 (2010) 8494–8502

Contents lists available at ScienceDirect

Tetrahedron

journal homepage: www.elsevier.com/locate/tet

Selective arylation of aldehydes with di-rhodium(II)/NHC catalysts

Alexandre F. Trindade [a], Vânia André [b], M. Teresa Duarte [b], Luís F. Veiros [b], Pedro M.P. Gois [c,*], Carlos A.M. Afonso [a,c,*]

[a] CQFM, Centro de Química-Física Molecular and IN—Institute of Nanosciences and Nanotechnology, Instituto Superior Técnico, 1049-001 Lisboa, Portugal
[b] CQE, Departamento de Engenharia Química e Biológica, Complexo I, Instituto Superior Técnico, Av. Rovisco Pais 1, 1049-001 Lisboa, Portugal
[c] iMed.UL, Faculdade de Farmácia da Universidade de Lisboa, Av. Prof. Gama Pinto, 1649-003 Lisboa, Portugal

ARTICLE INFO

Article history:
Received 25 May 2010
Received in revised form 16 July 2010
Accepted 18 August 2010
Available online 23 September 2010

Keywords:
Rhodium (II)
Catalysis
Arylation
Boronic acids
N-Heterocycliccarbenes (NHC)
Alcohol racemization
DFT calculations

ABSTRACT

Here is described the preparation of four new rhodium(II) complexes bearing axial NHC ligands. The presence of electron-withdrawing bridging ligands resulted in an enhanced reactivity in the arylation of aldehydes with boronic acids when compared with the tetraacetate counterparts. Complex **15** ($Rh_2tfa_4(IPr)_2$) proved to be the most active catalyst for this transformation allowing the selective conversion of aromatic, aliphatic and vinyl aldehydes into the respective alcohols in excellent yields. It was demonstrated that the good group tolerance could be further extended to aromatic and conjugated ketones. DFT calculations carried out on this system showed the complementarily of the bridging ligands and axial ligand in these dinuclear complexes. It was also disclosed that Rh(II)/NHC catalytic system can promote the racemization of 1-phenyl ethanol.

1. Introduction

Diarylmethanols are important structural motives in a multitude of pharmacologically active compounds and therefore represent an important synthetic target. In recent years the metal catalyzed C–C bond formation between aldehydes and boronic acids as become a very useful approach to prepare such compounds (Scheme 1).[1,2]

In 2001 Fürstner et al. developed an efficient protocol to perform the arylation of aldehydes using catalytic systems based on *N*-heterocyclic ligands (NHC) and rhodium complexes.[2j] Inspired by his work we initiated a program in order to elucidate if di-rhodium (II) complexes combined with NHC ligands could act as catalysts in this transformation. Apart from the catalytic performance we were particularly interested in understanding the axial ligand influence in the overall reactivity of these widely used dinuclear complexes.

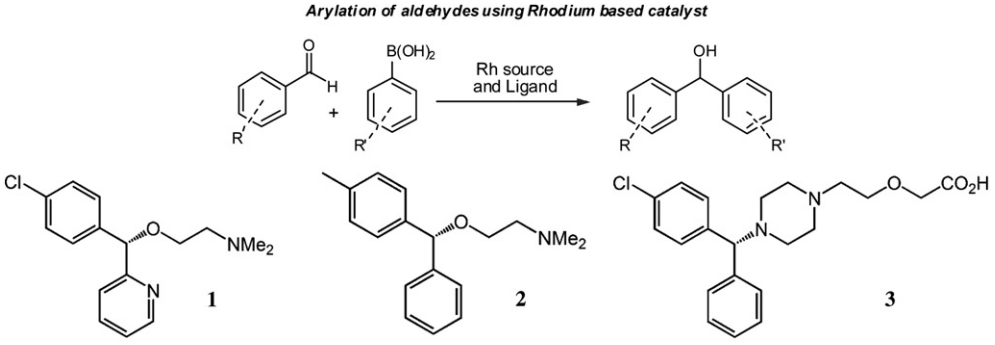

Scheme 1. General arylation of aldehydes using boronic acids and rhodium based catalysts and (below) examples of biologically active compounds derived from diarylmethanols: (*S*)-carbinoxamine **1** and Zyrtec **3** are H1 antagonists used for the treatment of allergic diseases, Orphenadrine **2** shows antihistaminic and anticholinergic activity.

* Corresponding authors. Fax: +351 21 846 4455/7 (C.A.M.A.); fax: +351 21 7946470 (P.M.P.G.); e-mail addresses: pedrogois@ff.ul.pt (P.M.P. Gois), carlosafonso@ist.utl.pt (C.A.M. Afonso).

0040-4020/$ – see front matter © 2010 Elsevier Ltd. All rights reserved.
doi:10.1016/j.tet.2010.08.050

In the course of our studies, we demonstrated that the NHC ligand binds axially to the di-rhodium (II) complex and efficiently tunes its reactivity allowing the arylation reaction to take place in high yields and selectivities. Based on DFT calculations and structural work we established that NHCs **4** and **5** are the preferential axial ligands, which confer high stereochemical protection around one of the Rh atoms at the same time that transfer charge through the Rh–Rh bond to the terminal rhodium centre.[3]

Furthermore, and differently from most arylations of aldehydes using boronic acids catalyzed by Rh(I) complexes, which are thought to proceed via a transmetallation step,[4] NHC/di-Rh(II) catalysts appear to activate the boronic acid via the direct coordination of this species onto the complex (Scheme 2).[3b]

In our previous studies we also observed that the di-Rh(II) complex bridging ligands play a crucial role in the kinetics of the arylation reaction. Complexes with bridging electron-withdrawing ligands, such as trifluoroacetate **14** or perfluorobutyrate **13** are more active than their counterparts **10**–**12** in protocols wherein the catalyst was prepared in situ (Table 1).[3a]

Despite this important observation, the synthesis and characterization of catalysts combining electron-withdrawing bridging ligands with axial σ-donating NHC ligands have not been reported yet and this constitutes the topic of this report.

2. Results and discussion

With the objective of understanding the impact of the combination of electron-withdrawing bridging ligands with the axial NHC ligand on the catalyst structure and efficiency, we prepared complexes **15** and **16** simply by heating $Rh_2(tfa)_4$ with the

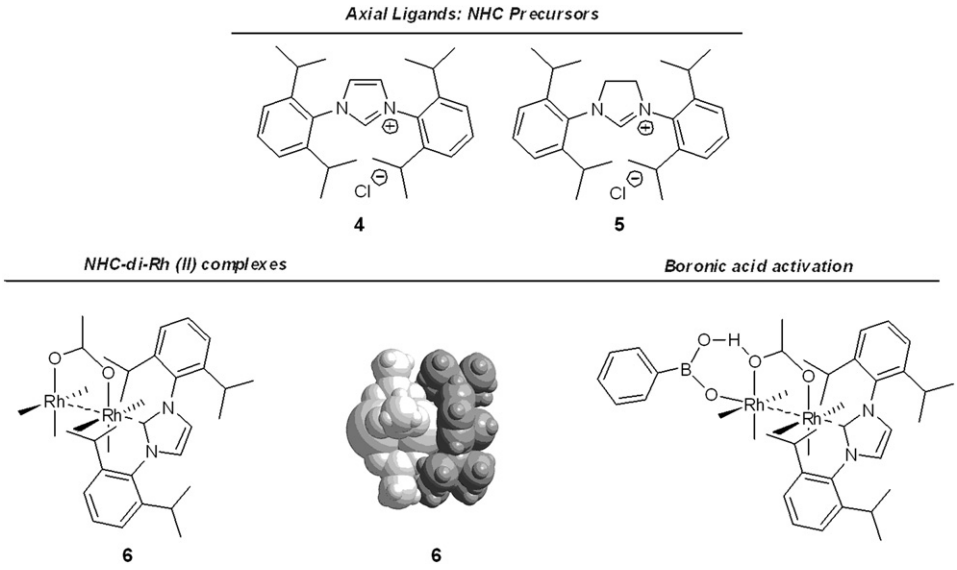

Scheme 2. New rhodium (II) catalysts developed and mechanistic rationalization for boronic acid activation.

Table 1
Di-rhodium(II) catalyst evaluation study (in situ method)[3b]

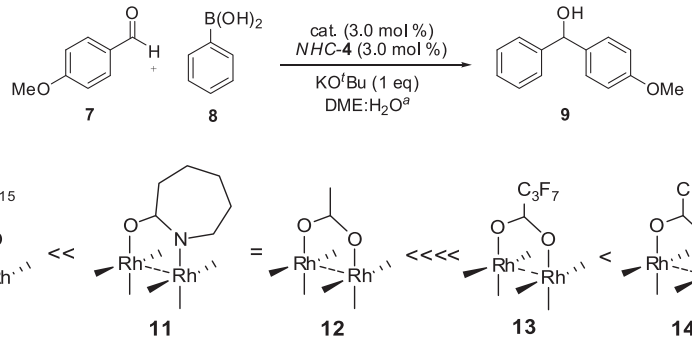

Entry	Cat.	Temp (°C)	Time (h)	Yield (%)[b]
1	**10**	90	6	92
2	**11**	90	0.5	90
3	**11**	60	24	n.r.
4	**12**	90	0.5	94
5	**12**	60	24	n.r.
6	**13**	90	0.5	95
7	**13**	60	24	83
8	**14**	60	24	90

[a] DME/H_2O (0.5:0.12 ml).
[b] Isolated yields after purification by preparative thin layer chromatography.
n.r.=no reaction.

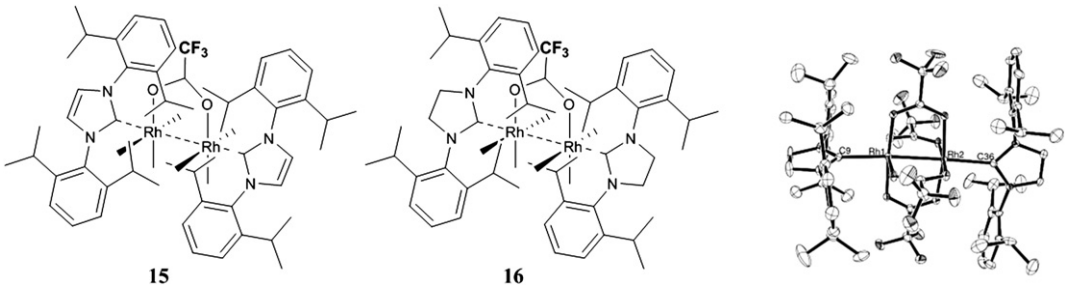

Scheme 3. Left: new complexes prepared; right: Complex **15**, ORTEP3.2[5] diagram (ellipsoids at 30% probability) of the di-Rh complex. Hydrogen atoms were excluded for clarity. Selected bond lengths are: Rh1–Rh2 2.496(2) Å, Rh1–C9 2.218(5) Å; Rh2–C36 2.245(5) Å. All the coordination angles are around 90°. In compound 15, one of the Rh–C distance (Rh1–C9) is slightly shorter than the other and the two carbenes are relatively rotated about 90°.

respective *N*-heterocyclic carbene in toluene. Differently from complex **16** suitable crystals for X-ray analysis of **15** were obtained after a toluene solution of **15** was left standing at −20 °C overnight (Scheme 3). Rather surprisingly and despite our efforts the corresponding mono-complexes were not obtained.

In addition to **15** and **16** we also prepared two new complexes **17** and **18** with electron-withdrawing substituents in the NHC backbone (Scheme 4). In this case, the mono-species **18** was easily prepared after eluting the parent complex **17** in a preparative thin layer chromatography. Suitable crystals for X-ray analysis of **17** were obtained after the toluene solution containing the complex was left standing at −20 °C overnight (Scheme 4).

It was expected that the presence of bridging ligands with electron-withdrawing character could make the NHC ligands more coordinated to the rhodium (relatively to complex **20**). If taken in account the bond distances of between Rh1–C9 and Rh2–C36 this hypothesis is correct. The shortest Rh–C bonds are observed for complex **15** (Table 2). In opposition, the introduction of electron-withdrawing groups in the NHC imidazolidene ring should attenuate its coordination ability, which is also true (comparing complex **17** to **20**, Table 2).

The formation of the Rh–NHC bond corresponds to electron transfer from the carbene to a Rh–Rh antibonding orbital of the metallic fragment, which results in a increased Rh–Rh distance.[3]

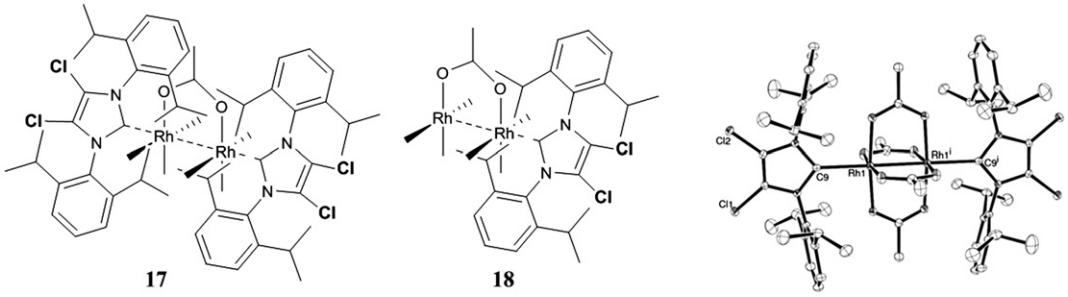

Scheme 4. Left: new complexes prepared; right: Complex **17**, ORTEP3.2[5] diagram (ellipsoids at 30% probability) of the di-Rh complex. Hydrogen atoms were excluded for clarity. Selected bond lengths are: Rh1–Rh1^{i} 2.451(3) Å, Rh1–C9 2.236(4) Å. All the coordination angles are around 90°.

It was seen in the past that the small structural differences between complexes **19** and **20** (Scheme 5 and Table 2) accounted for distinct catalytic behaviour for the arylation of aldehydes.[3b]

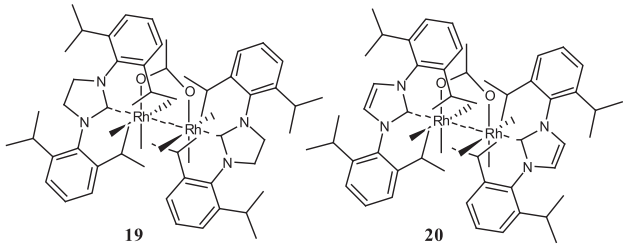

Scheme 5. NHC/di-Rh (II) dimers previously prepared.[3]

Table 2
Selected bond distances [Å] for compounds **15**, **17**, **19** and **20**

	15	**17**	**19**	**20**
Rh1–C9	2.218(5)	2.236(4)	2.244(7)	2.228(3)
Rh2–C36	2.245(5)	2.236(4)[a]	2.244(7)[a]	2.244(3)
Rh–Rh	2.496(2)	2.451(3)[a]	2.462(1)[a]	2.4731(3)
Rh–O	2.023–2.057	2.014–2.038	2.029–2.044	2.044–2.061

[a] Generated by symmetry.

This bond should be less sensitive to alterations due to the presence of the bridging ligands but, nevertheless they are present.

With complexes **15**–**18** in hand we carried out their catalytic evaluation in the arylation of *p*-methoxybenzaldehyde with phenylboronic acid. In our previous studies, we observed that complex **19** was to some extent more active than complex **20** in this reaction (Table 3, entries 1 and 2).[3b] Considering this subtle difference, we anticipated that the inclusion of electron-withdrawing substituents on the NHC backbone would affect the reactivity profile of these

Table 3
Catalyst and solvent screening for the arylation of *p*-methoxybenzaldehyde[a]

Entry	Catalyst	Temp (°C)	Solvent	Time (h)	Yield
1	**19**[b]	60	Methanol	5.5	94%
2	**20**[b]	60	Methanol	5.5	67%
3	**17**	60	Methanol	5	n.r.[d]
4	**18**	60	Methanol	5	Traces
5	**15**	60	Methanol	4	99%
6	**16**	60	Methanol	4	95%
7	$Rh_2(tfa)_4$[c]	60	Methanol	4	10%
8	**15**	60	*tert*-Amyl alcohol	4	n.r.[d]
9	**15**	60	DME/water[e]	4	n.r.[d]

[a] 0.25 mmol aldehyde, 0.025 mmol KO^{t}Bu, 0.5 mmol boronic acid, 0.5 ml solvent.
[b] Ref. 3b.
[c] tfa—trifluoroacetate.
[d] n.r.—no reaction.
[e] 5/1 Dimethoxyethane/water.

complexes. Rather surprisingly the chlorinated complexes **17** and **18** failed to give any arylated product (Table 3, entries 3 and 4). In this particular case the lack of reactivity is most likely due to NHC decoordination in the reaction conditions as the mixture rapidly exhibited a green colour indicating the presence of the parent $Rh_2(OAc)_4$. The axial ligand decoordination in complexes **18** was quite surprising to us and for that reason we performed DFT calculations on this system in order to establish how strongly the carbene is attached to the rhodium center (Scheme 6). Our calculations showed that in this mono-species the carbene is more weakly coordinated to the rhodium than in complex **6**. This interpretation can be rationalised by analyzing the strength of the Rh–C bond both in terms of distance and Wiberg Index.[6]

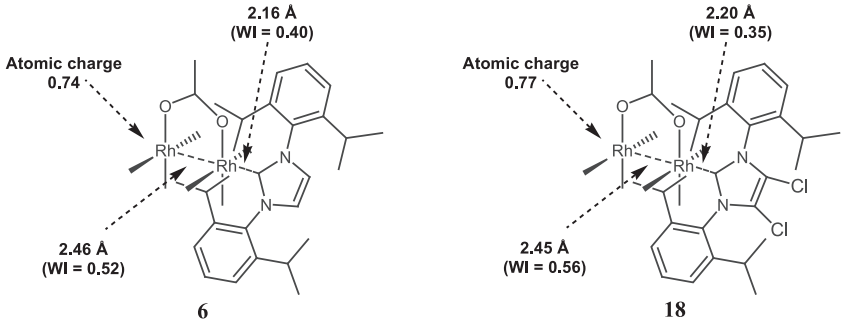

Scheme 6. Charge and bond analysis for complex **6** and **18**.

The Wiberg index of Rh–C bond in complex **6** is about 9% higher compared with the same bond of complex **18**, which results in a shorter bond length, a stronger bond (2.16 Å vs 2.20 Å, for complex **6** and **18**, respectively). The Rh–Rh bond distance is less sensitive to those variations because it is geometrically constrained by the bridging ligands (2.46 Å vs 2.45 Å, for complex **6** and **18**, respectively). Therefore the inclusion of chlorides in the backbone of the NHC resulted in a less stable catalyst, which rapidly lost catalytic efficiency in the reaction conditions due to NHC displacement.

Performing the reaction using complexes **15** and **16** with electron-withdrawing bridging ligands, secondary alcohol was obtained almost quantitatively at 60 °C (Table 3, entries 5 and 6). These results indicated that these complexes display a higher activity than the previously prepared dimers **19** and **20**. A control experiment was conducted using $Rh_2(tfa)_4$ as catalyst, proving that the *N*-heterocyclic carbene truly has a rate accelerating effect in these catalytic systems (Table 3, entry 7). Exploring the reaction conditions, we observed that other solvent systems apart from methanol were less efficient for the process (Table 3, entries 8 and 9).

Once confirmed the high activity of complex **15**, the protocol was extended to a variety of aldehydes (Table 4). Differently from what occurs when using standard Rh(I) complexes,[2] the arylation of

Table 4
Product scope in arylation of aliphatic, aromatic and allylic aldehydes using complex **15**[a]

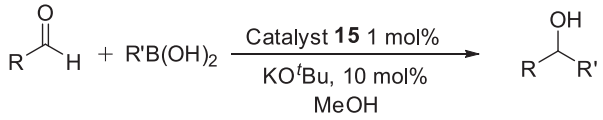

Entry	Aldehyde	Boronic Acid	Temp (°C)	Product	Time (h)	Yield (%)
1	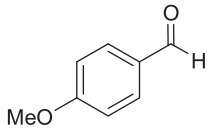 **7**	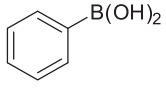 **8**	60	**9**	4	99
2	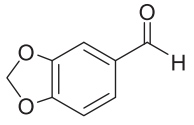 **21**	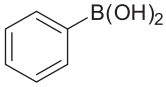 **8**	60	**33**	7	90
3	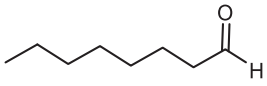 **22**	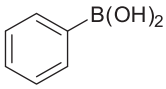 **8**	60	**34**	7	99
4	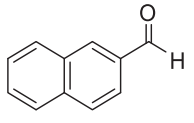	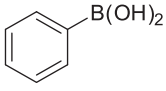 **8**	65	**35**	4	99
5	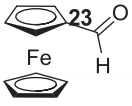 **24**	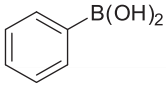 **8**	65	**36**	4	96

(*continued on next page*)

Table 4 (*continued*)

Entry	Aldehyde	Boronic Acid	Temp (°C)	Product	Time (h)	Yield (%)
6	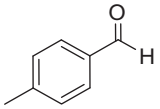 **25**	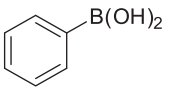 **8**	65	**37**	3	98
7	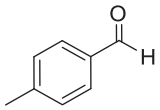 **26**	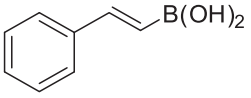 **31**	65	**38**	4	97
8	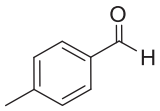 **27**	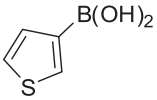 **32**	65	**39**	18	89
9	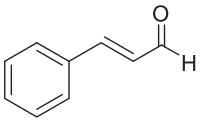 **28**	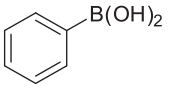 **8**	65	**40**	6	95
10	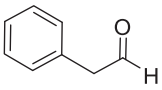 **29**	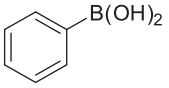 **8**	65	**41**	4	92
10	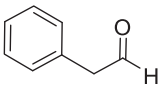 **29**	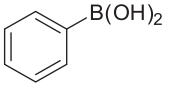 **8**	65	**41**	4	92

[a] 0.25 mmol aldehyde, 0.025 mmol KO^{t}Bu, 0.5 mmol boronic acid, 0.5 ml MeOH

electron-rich aldehydes is preferentially achieved when using NHC/Rh(II) catalysts (Table 4, entries 1 and 2). The protocol was highly successful in the arylation of a variety of aryl aldehydes (Table 4, entries 4–8) using different boronic acids. Alkyl aldehydes, which can easily undergo aldol condensations, were also selectively transformed into the corresponding alcohol in yields up to 99% (Table 4, entries 3 and 10). Finally, catalyst **15** exclusively afforded 1,2-addition product when a α,β-conjugated aldehyde was used as substrate (Table 4, entry 9).

Interestingly, when using thienyl boronic acid to perform the arylation of *p*-tolualdehyde, a considerable longer reaction time was required to achieve a higher yield of secondary alcohol (Table 4,

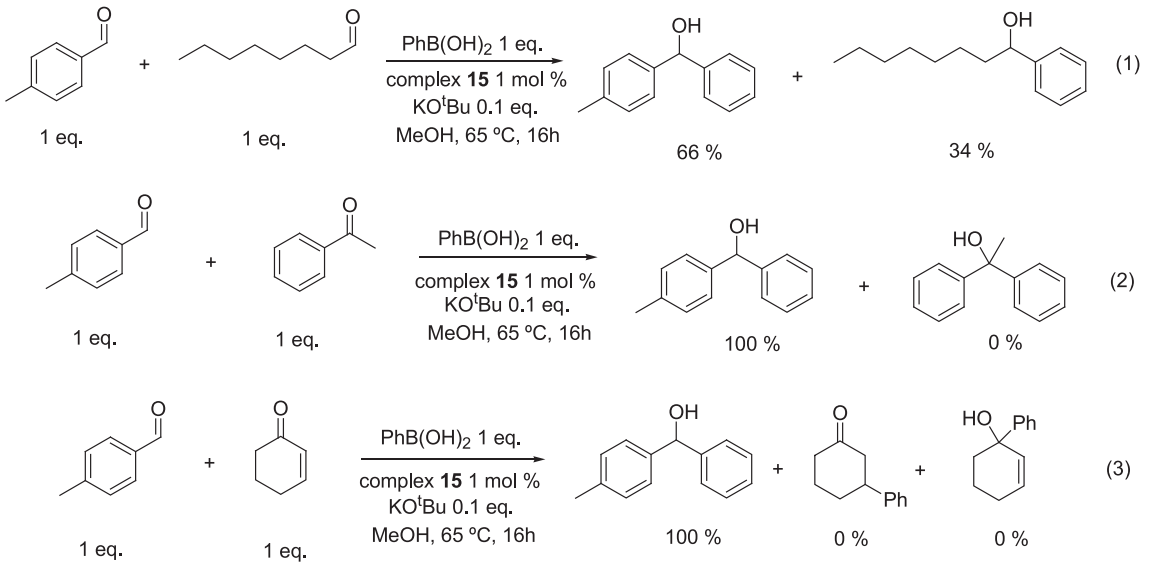

Scheme 7. Competitive experiments with complex **15**.

Table 5
DFT calculated electronic properties in the active species of complexes **15**, **16**, **19** and **20**. Rh2 is directly attached to NHC; B3PW91/VDZP

Active species of complex	Total charge in Rh_2	Charge in bridging ligands	Charge in NHC	Atomic charge Rh1	Atomic charge Rh2	Wiberg Index Rh1–Rh2	Wiberg Index Rh2–C
15	1.63	−1.97	0.35	0.73	0.90	0.48	0.43
16	1.63	−1.97	0.35	0.73	0.90	0.49	0.43
19	1.63	−1.91	0.28	0.74	0.89	0.52	0.40
20	1.63	−1.91	0.28	0.74	0.89	0.52	0.40

entry 8). This fact is probably related with competitive axial coordination of sulfur, which inhibits the boronic acid hydroxyl group attachment to this position as shown in Scheme 2.

This methodology was shown to be quite efficient towards the arylation of aldehydes bearing electro donating substituents and alkyl aldehydes. Considering the results displayed in Table 4, aryl aldehydes appear to be more reactive than alkyl aldehydes. This was further demonstrated when a competitive reaction was conducted with both types of aldehydes with only 1 equiv of boronic acid (Scheme 7, Eq. 1). The product derived from the arylation of *p*-tolualdehyde was preferentially formed in a ratio of 2/1.

Additional competitive experiments were conducted in order to understand the selectivity profile of this protocol. When acetophenone and 1-cyclohex-2-enone were used in equi-stoichiometric amounts relative to *p*-tolualdehyde only the aldehyde was converted to the diarylmethanol and no products resulting from the 1,2- and/or 1,4- addition to 1-cyclohex-2-enone were detected. These series of reactions highlight the high preference of this protocol towards the arylation of aldehydes, which may be conducted in a highly selectively manner in the presence of aromatic and α,β-unsaturated ketones.

As mentioned previously, the presence or absence of saturation in the NHC ring proved in the past to be responsible for distinct catalytic abilities.[3] Herein, the presence of saturation on complex **16** had little effect on the overall activity of the catalyst comparing with catalyst **15** (Table 3, entries 5 and 6). To further understand the relationship between both ligands we analyzed several electronic properties in the active species of complexes **15**, **16**, **19** and **20** (Table 5 and Scheme 6).

Table 5 and Scheme 6 present the charge distribution calculated by means of a Natural Population Analysis, NPA,[7] for several fragments of the relevant species (the two metal atoms, the four bridging ligands, and the NHC ligand). Although the calculated charges cannot provide a full explanation of the reactivity differences observed experimentally, some interesting conclusions can be drawn. As we shift from the molecules with acetate bridges (complexes **19** and **20**) to the trifluoroacetate species (complexes **15** and **16**), the NHC donates more charge (and becomes more positive), while this is compensated by the bridging ligands, that receive the extra electron density and become more negative. The flow of charge along the complex is represented in Scheme 8. By this way, the rhodium centers have a passive behaviour, and the Rh_2 fragment remains with the same charge in all species.

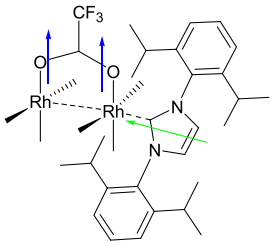

Scheme 8. Equatorial vs axial ligands effect.

The electron flow observed from the NHC to the bridging ligands has a direct effect on both the Rh–Rh and the Rh–NHC bonds. The NHC is forced to donate more electron density in the complexes with fluorinated bridges, strengthening the Rh–NHC bond and, at the same time, weakening the Rh–Rh bond, given the Rh–Rh σ* nature of

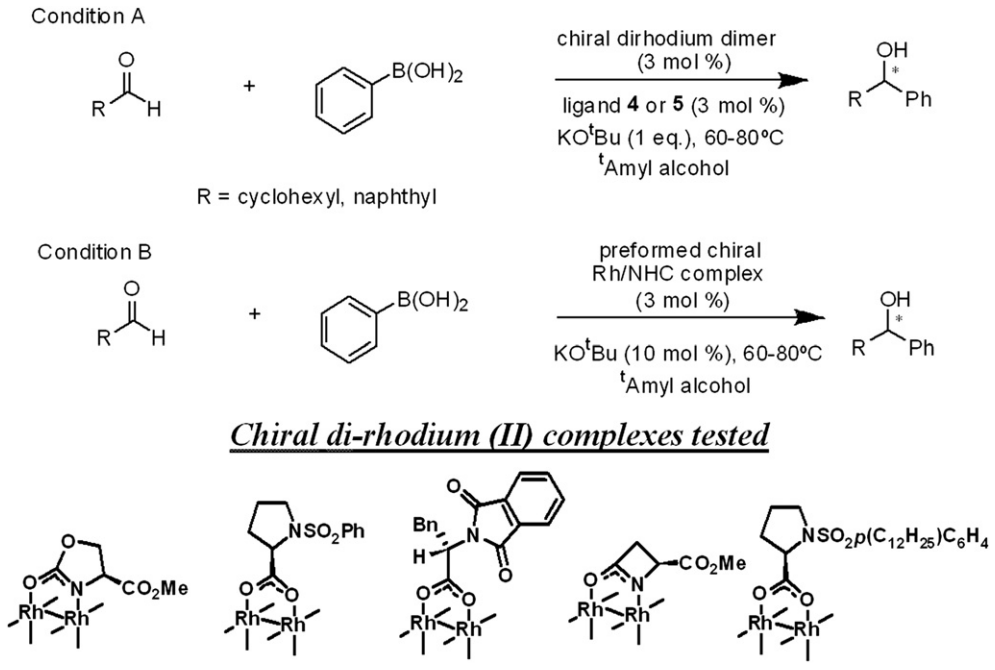

Scheme 9. Chiral approaches studied for arylation of aldehyde.

the metal fragment orbital involved in the Rh–NHC bond.[3a,8] These features are fully demonstrated by the Wiberg indices presented in Table 5. It should be noticed that, although a clear trend is presented, these results must be taken with caution given the small differences of the calculated charges. The bridging ligands tend to hold at the same distance the Rh atoms, thus making the Rh–Rh bond distance less sensitive to charge variations in the complex.

Following our mechanistic proposal (see Scheme 2) we envisioned the possibility to prepare enantioenriched secondary alcohols[9] performing the reaction with di-rhodium (II) complexes bearing chiral bridging ligands and the axial NHC ligand. Therefore, we tested several commercially available chiral di-rhodium dimmers with recognized efficiency in traditional di-rhodium (II) chemistry[10] (eg, C–H insertions reactions of diazo compounds), in the arylation of aldehydes. Surprisingly, when performing the reaction either via the in situ methodology (condition A, Scheme 9) or using the pre-synthesised NHC ligand (condition B, Scheme 9) only racemic alcohols were obtained (Scheme 9).

In 1996 Williams et al. showed that a mixture of $Rh_2(OAc)_4$/phenanthroline and acetophenone promoted the racemization of 1-phenyl ethanol.[11] Regarding this precedent we envisioned that our NHC/Rh(II) system could also be involved in the secondary aryl alcohols racemization, explaining in this way the non existence of enantiomeric excess when using chiral di-rhodium (II) complexes. This was confirmed when we reacted enantiopure 1-phenyl ethanol with our NHC/Rh (II) complexes. When using catalyst **6** it was possible to fully racemize enantiopure 1-phenyl ethanol in 2 h only in the presence of KO^{t}Bu (Fig. 1).

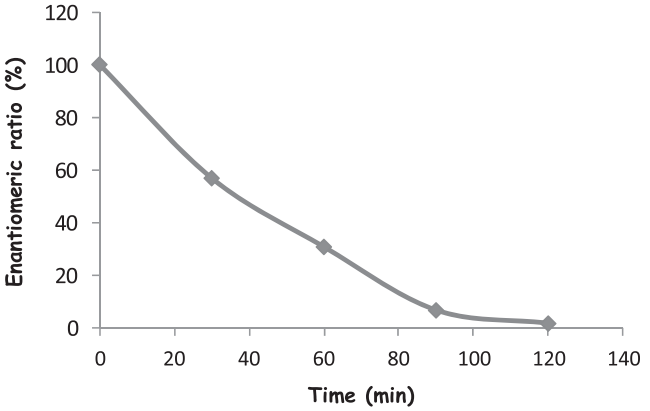

Fig. 1. Racemization of (*S*)-1-phenyl ethanol in presence of catalyst **6**.

3. Conclusion

In summary, we were able to prepare a new family of rhodium (II) complexes bearing NHC ligands in the axial coordination site. The presence of electron-withdrawing bridging ligand provided the best catalysts for this transformation, while the introduction of electron-withdrawing groups in the imidazolidene leads to inactive catalysts due to ligand decoordination.

Complex **15** was able to catalyze the arylation of aldehydes with boronic acids with high efficiency and considerably high group tolerance. This group tolerance could be further extended to aromatic and conjugated ketones since they proved to be non reactive under the conditions presented in this work. It was demonstrated that aromatic aldehydes with electron donating substituents react in more extension than alkyl aldehydes.

Studies towards the asymmetric arylation reactions allowed us to discover that this catalytic system is also able to promote quite efficiently the racemization of 1-phenyl ethanol.

4. Experimental

4.1. General remarks

1,2-Dimethoxyethane (DME), acetonitrile (CH_3CN), toluene and *tert*-amyl alcohol were freshly distilled over calcium hydride prior to use. Ethyl acetate was distilled over potassium carbonate, while methanol was distilled from magnesium. Tetrahydrofuran was dried and freshly distilled over sodium/benzophenone. Tetrachlorocarbon was used without any purification. Flash chromatography was carried out on silica gel 60 M purchased from MN (Ref. 815381), preparative thin layer chromatography plates were prepared with silica gel 60 GF_{254} MercK (Ref. 1.07730.1000). Reaction mixtures were analyzed by TLC using ALUGRAM® SIL G/UV_{254} from MN (Ref. 818133, silica gel 60), and visualisation of TLC spots was effected using UV and phosphomolybdic acid solution. NMR spectra were recorded in a Bruker AMX 400 using $CDCl_3$ and $C_6D_5CD_3$ as solvent and $(CH_3)_4Si$ (^1H) as an internal standard. All coupling constants are expressed in hertz. Di-rhodium catalysts were purchased from Aldrich: $Rh_2(OAc)_4$—Rhodium (II) acetate dimer; $Rh_2(tfa)_4$—Rhodium (II) trifluoroacetate dimmer. Potassium *tert*-butoxide was purified by sublimation and stored under Argon before use.

NHC ligands used were prepared following reported procedures: 1,3-bis(2,6-diisopropylphenyl) imidazolium chloride, 1,3-bis(2,6-diisopropylphenyl) imidazolinium chloride and 1,3-bis-(2,6-diisopropylphenyl)-4,5-dichloroimidazol-2-ylidene.[12] The aldehydes, boronic acids and CCl_4 were purchased from Aldrich and used without further purification.

High Pressure Liquid Chromatography for the enantiomeric excess determination was carried out using a Dionex P680 pump equipped with a diode array detector and Chiralcel OD column.

4.2. Synthesis and characterization of complex 15

Rhodium trifluoroacetate (50 mg, 0.076 mmol) was added to a flame dried Schlenk and suspended in freshly distilled and dried toluene (4 ml). To this mixture was added 1,3-bis-(2,6-diisopropylphenyl)-imidazol-2-ylidene[12] (62 mg, 0.160 mmol). This mixture was heated under 80 °C until the solution turned to red wine colour (about 2 h). The volume was concentrated and the desired complex was obtained as an orange powder in 80% yield (80 mg). Further recrystallizations from toluene afforded orange single crystals suitable for X-ray crystallography.

^1H NMR (C_7D_8) δ (ppm)=7.27–6.99 (m, toluene), 6.67 (s, 4H), 3.37–3.30 (m, 8H), 2.15–2.11 (toluene), 1.18 (d, 24H, J=6.6 Hz), 1.04 (d, 24H, J=6.6 Hz); ^{13}C NMR (C_7D_8) δ (ppm)=144.77, 137.79, 129.08, 128.91, 123.40, 27.96, 25.06, 22.42, 22.24. ^{19}F NMR (C_7D_8) δ (ppm)=−73.49. MS (FAB^+): m/z=1434.0, 487.0, 389.2. HMRS (FAB^+): m/z calcd 1434.3263; found 1434.3323. Mp: 250 °C (degrad.)

Crystallographic data for complex **15**: $C_{62}H_{72}F_{12}N_4O_8Rh_2$, fw=1435.06, monoclinic, space group $P2_1/c$, a=18.819(7) Å, b=16.401(6) Å, c=23.035(8) Å, β=95.759(2)°, V=7074(4) Å^3, Z=4, T=150 K, ρ_{calcd}=1.347 mg m^{-3}, μ=0.548 mm^{-1}, F(000)=2936, red crystal (0.18×0.13×0.04 mm). Of 1,07,672 reflections collected, 14,381 were independent (Rint=0.1746); 811 variables refined with 14381 reflections to final R indices R_1=0.0596, wR_2 (all data)=0.1482, GOF=0.962.

The diffraction data for this complex is poor due to its low diffraction and quality of the crystals.

4.3. Synthesis and characterization of complex 16

Rhodium trifluoroacetate (50 mg, 0.076 mmol) was added to a flame dried Schlenk and suspended in freshly distilled and dried toluene (4 ml). To this mixture was added 1,3-bis-(2,6-diisopropylphenyl)-imidazolin-2-ylidene[12] (63 mg, 0.160 mmol). This

mixture was heated under 80 °C until the solution turned to red wine colour (about 2 h). The volume was concentrated and the desired complex was obtained as an orange powder in 70% yield (71 mg). Due to some instability it was not possible to obtain this complex free of impurities by recrystallization after the reaction. The presence of impurities can be detected in ^{1}H NMR.

^{1}H NMR (C_7D_8) δ (ppm)=7.27–6.97 (m, toluene), 3.78 (s), 3.64–3.60 (m), 2.09–2.08 (toluene), 1.28–1.06 (dd); ^{13}C NMR (C_7D_8) δ (ppm)=147.62, 142.00, 129.34, 128.92, 123.58, 49.40, 28.19, 27.71, 24.12. ^{19}F NMR (C_7D_8) δ (ppm)=−73.96.

4.4. Synthesis and characterization of complex 17

Rhodium tetraacetate (50 mg, 0.11 mmol) was added to a flame dried Schlenk and suspended in freshly distilled and dried toluene (4 ml). To this mixture was added 1,3-bis-(2,6-diisopropylphenyl)-4,5-dichloroimidazol-2-ylidene[12] (110 mg, 0.24 mmol). This mixture was heated under 80 °C until the solution turned to red wine colour (about 2 h). The volume was concentrated and the desired complex was obtained as an orange powder in 90% yield (130 mg). Further recrystallizations from toluene afforded orange single crystals suitable for X-ray crystallography.

^{1}H NMR (C_7D_8) δ (ppm)=7.21–7.01 (m, toluene), 3.40–3.35 (m, 4H), 2.14–2.11 (m, toluene), 1.28 (d, 12H, J=6.6 Hz), 1.04 (br d, 18H, J=6.6 Hz); ^{13}C NMR (C_7D_8) δ (ppm)=189.23, 146.60, 137.09, 135.20, 129.09, 122.93, 118.76, 28.13, 23.88, 23.17, 20.80. MS (FAB$^+$): m/z=1356.9, 897.9. Anal. Calcd for $C_{62}H_{72}Cl_4N_4O_8Rh_2$: C, 54.88; H, 5.94; N, 4.13. Found: C, 54.87; H, 6.05; N, 4.11. Mp: 250 °C (degrad.)

Crystallographic data for complex **17**: $C_{62}H_{80}C_{l4}N_4O_8Rh_2$, fw=1356.92, monoclinic, space group C_2/c, a=29.3020(7) Å, b=11.4810(4), c=21.0850(5) Å, β=101.332(6)°, V=6955.1(3) Å^3, Z=4, T=150 K, ρ_{calcd}=1.296 mg m^{-3}, μ=0.678 mm^{-1}, F(000)=2808, orange crystal (0.45×0.30×0.20 mm). Of 69,787 reflections collected, 12,144 were independent (Rint=0.1333); 372 variables refined with 12144 reflections to final R indices R_1=0.0458, wR_2 (all data)=0.1097, GOF=0.932.

4.5. Synthesis and characterization of complex 18

Complex **17** (0.150 g, 1.11×10^{-1} mmol) was eluted by preparative thin layer chromatography (30% ethyl acetate in hexanes) yielding the respective mono-complex **18** (0.084 g, 85% yield). The mono-complex formation is observed by immediately change of colour from orange to purple colour in the plate.

^{1}H NMR (C_7D_8) δ (ppm)=7.13–6.99 (m, toluene), 3.29–3.24 (m, 4H), 2.15–2.12 (toluene), 1.34 (br s, 12H), 1.25 (d, 12H, J=6.6 Hz), 1.08 (d, 12H, J=6.6 Hz); ^{13}C NMR (C_7D_8) δ (ppm)=188.57, 146.27, 137.40, 134.51, 129.68, 123.25, 119.23, 28.33, 23.91, 23.41, 22.70. MS (FAB$^+$): m/z=897.9, 457.1. HMRS (FAB$^+$): m/z calcd 898.0741; found 898.0745. Mp: 250 °C (degrad.)

4.6. General procedure for the catalyst and solvent screening in arylation of *p*-methoxybenzaldehyde; Table 3

Catalyst (2.50×10^{-3} mmol, 1 mol %) was weighted into a flamed dried round bottom flask equipped with a condenser and under argon atmosphere. Solvent (0.5 ml) was added and the suspension was stirred at room temperature for 5 min then, phenylboronic acid (61.00 mg, 0.50 mmol, 2 equiv), KO^{t}Bu (2.80 mg, 2.5×10^{-2} mmol, 10 mol %). In case of the reaction using DME/water as solvent system, the water is added before the 4-methoxybenzaldehyde (34.00 mg, 0.25 mmol). The resulting mixture was stirred at 60 °C for different periods of time. The end of the reaction was determined by TLC analysis when the aldehyde was fully consumed. The reaction mixture was concentrated under reduced pressure and the residue was purified by preparative thin layer chromatography (ethyl acetate/hexane), yielding the desired secondary alcohol as a slightly yellow oil, which crystallized upon standing at low temperature (fridge).

4.7. General procedure for the substrate scope in arylation of aliphatic, aromatic and allylic aldehydes using complex 15; Table 4

Complex **15** (3.60 mg, 2.50×10^{-3} mmol, 1 mol %) was weighted into a flamed dried round bottom flask equipped with a condenser and under argon atmosphere. Methanol (0.5 ml) was added and the suspension was stirred at room temperature for 5 min then, boronic acid (0.50 mmol, 2 equiv), KO^{t}Bu (2.80 mg, 2.5×10^{-2} mmol, 10 mol %), followed by the desired aldehyde (0.25 mmol). The resulting mixture was stirred at 60 °C or 65 °C for different periods of time depending on the reactants. The end of the reaction was determined by TLC analysis when the aldehyde was fully consumed. The reaction mixture was concentrated under reduced pressure and the residue was purified by preparative thin layer chromatography (ethyl acetate/hexane), yielding the desired secondary alcohol as a slightly yellow oil, which crystallized upon standing at low temperature (fridge).

4.8. General procedure for competitive experiments

Complex **15** (3.60 mg, 2.50×10^{-3} mmol, 1 mol %) was weighted into a flamed dried round bottom flask equipped with a condenser and under argon atmosphere. Methanol (0.5 ml) was added and the suspension was stirred at room temperature for 5 min then, phenylboronic acid (0.25 mmol, 1 equiv), KO^{t}Bu (2.80 mg, 2.5×10^{-2} mmol, 10 mol %), followed by the desired equimolar amounts of aldehydes or aldehyde and ketone. The resulting mixture was stirred at 65°C for 16 h. The crude reaction was analyzed by TLC and NMR.

4.9. General procedure for the enantioselective arylation reactions by conditions A

Chiral Rh (II) catalyst (7.50×10^{-3} mmol, 3 mol %) was weighted into a flamed dried round bottom flask equipped with a condenser and under argon atmosphere. *tert*-Amyl alcohol (0.5 ml) was added and the suspension was stirred at room temperature for 5 min. Then, phenylboronic acid (61.00 mg, 0.50 mmol), ligand **4** or **5** (7.50×10^{-3} mmol, 3 mol %), KO^{t}Bu (28.00 mg, 0.25 mmol) and aldehyde (0.25 mmol) were successively added. The resulting mixture was stirred at 60 or 80 °C for different periods of time (2–6 h). The reaction mixture was concentrated under reduced pressure and the residue was purified by preparative thin layer chromatography (ethyl acetate/hexane), yielding the desired secondary alcohol, which crystallized upon standing at low temperature (fridge). The residue was analyzed by chiral HPLC.

4.10. General procedure for the enantioselective arylation reactions by conditions B

Ligand **4** or **5** (7.50×10^{-3} mmol, 3 mol %) and KO^{t}Bu (2.80 mg, 10 mol %) were reacted in THF to 2 h. Then, the solvent was evaporated and the residue dissolved in dry toluene (1 ml) and added (filtration through Celite) to a solution of chiral Rh (II) catalyst (7.50×10^{-3} mmol, 3 mol %) in toluene (1 ml). The colour change occurs readily upon heating at 60 °C, indicating the coordinating of the ligand. The solvent is removed under reduced pressure and the catalyst dissolved in *tert*-amyl alcohol (0.5 ml). Then, phenylboronic acid (61.00 mg, 0.50 mmol), KO^{t}Bu (2.80 mg, 10 mol %) and aldehyde (0.25 mmol) were successively added. The resulting mixture was stirred at 60 or 80 °C for different periods of time (2–6 h). The reaction mixture was concentrated under reduced pressure and the residue was purified by preparative thin layer chromatography

(ethyl acetate/hexane), yielding the desired secondary alcohol, which crystallized upon standing at low temperature (fridge). The residue was analyzed by chiral HPLC.

4.11. General procedure for the kinetic studies of the racemization reaction

To a solution of complex **6** (1 mol %) in *tert*-amyl alcohol (2.5 ml), was added KO^{t}Bu (10 mol %) and 1-phenyl ethanol (1 equiv). The mixture was allowed to react at 80 °C and samples were collected at the given times and analyzed by chiral HPLC. Chiralcel OD column, eluent: 10% isopropanol in hexane, acetophenone R_f=6.6 min, (*R*)-1-phenyl ethanol R_f=10.2 min and (*S*)-1-phenyl ethanol R_f=12.9 min.

4.12. Computational details

Calculations were performed using the Gaussian 98 software package[13] and the B3PW91 hybrid functional, without symmetry constraints. That functional includes a mixture of Hartree–Fock[14] exchange with DFT exchange-correlation,[15] given by Becke's three parameter functional[16] with Perdew and Wang's 1991 gradient-corrected correlation functional.[17] The LanL2DZ basis set[18] augmented with an f-polarization function[19] was used for Rh, and a standard 6-31G(d,p)[20] for the remaining elements. A Natural Population Analysis (NPA)[7] and the resulting Wiberg indices[6] were used for a detailed study of the electronic structure and bonding of the optimized species. Atomic coordinates for all optimized structure are in the Supplementary data.

4.13. Crystallographic data

Crystallographic data (excluding structure factors) for the structure(s) reported in this paper have been deposited with the Cambridge Crystallographic Data Centre as supplementary publication no. CCDC 741791 and CCDC 741792. Copies of the data can be obtained free of charge on application to CCDC, 12 Union Road, Cambridge CB2 1EZ, UK [fax.: (internet.) +44 1223/336 033; e-mail: deposit@ccdc.cam.ac.uk].

Acknowledgements

We thank to FCT (POCI 2010) and FEDER (SFRH/BD/30619/2006, PTDC/QUI/66695/2006, and PTDC/QUI/66015/2006) for financial support.

Supplementary data

Supplementary data associated with this article can be found in online version at doi:10.1016/j.tet.2010.08.050. These data include MOL files and InChIKeys of the most important compounds described in this article.

References and notes

1. (a) Fagnou, K.; Lautens, M. *Chem. Rev.* **2003**, *103*, 169; (b) Bolm, C.; Hildebrand, J. P.; Muñiz, K.; Hermanns, N. *Angew. Chem., Int. Ed.* **2001**, *40*, 3284.
2. (a) Schmidt, F.; Stemmler, R. T.; Rudolph, J.; Bolm, C. *Chem. Soc. Rev.* **2006**, *35*, 454; (b) Lerebours, R.; Wolf, C. *J. Am. Chem. Soc.* **2006**, *128*, 13052; (c) Muramatsu, Y.; Harada, T. *Chem.—Eur. J.* **2008**, *14*, 10560; (d) Liao, Y.-X.; Xing, C.-H.; He, P.; Hu, Q.-S. *Org. Lett.* **2008**, *10*, 2509; (e) Yamamoto, Y.; Kurihara, K.; Miyaura, N. *Angew. Chem., Int. Ed.* **2009**, *48*, 4414; (f) Zou, T.; Pi, S.-S.; Li, J.-H. *Org. Lett.* **2009**, *11*, 453; (g) Zheng, H.; Zhang, Q.; Chen, J.; Liu, M.; Cheng, S.; Ding, J.; Wu, H.; Su, W. *J. Org. Chem.* **2009**, *74*, 943; (h) Arao, T.; Kondo, K.; Aoyama, T. *Tetrahedron Lett.* **2007**, *48*, 4115; (i) Biswas, K.; Prieto, O.; Goldsmith, P. J.; Woodward, S. *Angew. Chem., Int. Ed.* **2005**, *44*, 2232; (j) Fürstner, A.; Krause, H. *Adv. Synth. Catal.* **2001**, *343*, 343; (k) Bolm, C.; Muñiz, K. *Chem. Commun.* **1999**, 1295; (l) Bolm, C.; Hermanns, N.; Hildebrand, J. P.; Muñiz, K. *Angew. Chem., Int. Ed.* **2000**, *39*, 3465.
3. (a) Góis, P. M. P.; Trindade, A. F.; Veiros, L. F.; André, V.; Duarte, M. T.; Afonso, C. A. M.; Caddick, S.; Cloke, F. G. N. *Angew. Chem., Int. Ed.* **2007**, *46*, 5750; (b) Trindade, A. F.; Góis, P. M. P.; Veiros, L. F.; André, V.; Duarte, M. T.; Afonso, C. A. M.; Caddick, S.; Cloke, F. G. N. *J. Org. Chem.* **2008**, *73*, 4076.
4. Zhao, P.; Incarvito, C. D.; Hartwig, F. *J. Am. Chem. Soc.* **2007**, *129*, 1876.
5. Farrugia, L. *J. Appl. Crystallogr.* **1997**, *30*, 565.
6. (a) Wiberg, K. B. *Tetrahedron* **1968**, *24*, 1083.Wiberg indices are electronic parameters related to the electron density between atoms. They can be obtained from a Natural Population Analysis and provide an indication of the bond strength.
7. (a) Carpenter, J. E.; Weinhold, F. J. *Mol. Struct. (Theochem)* **1988**, *169*, 41; (b) Carpenter, J.E. PhD Thesis, University of Wisconsin Madison WI, 1987; (c) Foster, J. P.; Weinhold, F. *J. Am. Chem. Soc.* **1980**, *102*, 7211; (d) Reed, A. E.; Weinhold, F. J. *Chem. Phys.* **1983**, *78*, 4066; (e) Reed, A. E.; Weinhold, F. J. *Chem. Phys.* **1983**, *78*, 1736; (f) Reed, A. E.; Weinstock, R. B.; Weinhold, F. J. *Chem. Phys.* **1985**, *83*, 735; (g) Reed, A. E.; Curtiss, L. A.; Weinhold, F. *Chem. Rev.* **1988**, *88*, 899; (h) Weinhold, F.; Carpenter, J. E. *The Structure of Small Molecules and Ions*; Plenum: New York, NY, 1988; p 227.
8. Lloret, J.; Carbó, J. J.; Bo, C.; Lledós, A.; Pérez-Prieto, J. *Organometallics* **2008**, *27*, 2873.
9. For examples of enantioselective rhodium catalyzed aldehydes arylations reactions see: (a) Duan, H. F.; Xie, J. H.; Shi, W. J.; Zhang, Q.; Zhou, Q. L. *Org. Lett.* **2006**, *8*, 1479; (b) Jagt, R. B. C.; Toullec, P. Y.; de Vries, J. G.; Feringa, B. L.; Minnaard, A. J. *Org. Biomol. Chem.* **2006**, *4*, 773; (c) Martina, S. L. X.; Jagt, R. B. C.; de Vries, J. G.; Feringa, B. L.; Minnaard, A. J. *Chem. Commun.* **2006**, 4093; (d) Nishimura, T.; Kumamoto, H.; Nagaosa, M.; Hayashi, T. *Chem. Commun.* **2009**, 5713; (e) Noel, T.; Vandyck, K.; Van der Eycken, J. *Tetrahedron* **2007**, *63*, 12961.
10. (a) Davies, H. M. L.; Beckwith, R. E. J. *Chem. Rev.* **2003**, *103*, 2861; (b) Góis, P. M. P.; Afonso, C. A. M. *Eur. J. Org. Chem.* **2004**, 3773.
11. Dinh, P. M.; Howarth, J. A.; Hudnott, A. R.; Williams, J. M. J.; Harris, W. *Tetrahedron Lett.* **1996**, *37*, 7623.
12. Arduengo, A. J., III; Krafczyk, R.; Schmutzer, R.; Craig, H. A.; Goerlich, J. R.; Marshall, W. J.; Unverzagt, M. *Tetrahedron* **1999**, *55*, 14523.
13. Frisch, M. J.; Trucks, G. W.; Schlegel, H. B.; Scuseria, G. E.; Robb, M. A.; Cheeseman, J. R.; Zakrzewski, V. G.; Montgomery, J. A., Jr.; Stratmann, R. E.; Burant, J. C.; Dapprich, S.; Millam, J. M.; Daniels, A. D.; Kudin, K. N.; Strain, M. C.; Farkas, O.; Tomasi, J.; Barone, V.; Cossi, M.; Cammi, R.; Mennucci, B.; Pomelli, C.; Adamo, C.; Clifford, S.; Ochterski, J.; Petersson, G. A.; Ayala, P. Y.; Cui, Q.; Morokuma, K.; Malick, D. K.; Rabuck, A. D.; Raghavachari, K.; Foresman, J. B.; Cioslowski, J.; Ortiz, J. V.; Stefanov, B. B.; Liu, G.; Liashenko, A.; Piskorz, P.; Komaromi, I.; Gomperts, R.; Martin, R. L.; Fox, D. J.; Keith, T.; Al-Laham, M. A.; Peng, C. Y.; Nanayakkara, A.; Gonzalez, C.; Challacombe, M.; Gill, P. M. W.; Johnson, B. G.; Chen, W.; Wong, M. W.; Andres, J. L.; Head-Gordon, M.; Replogle, E. S.; Pople, J. A. *Gaussian 98, Revision A.7*; Gaussian,: Pittsburgh, PA, 1998; and provide an indication of the bond strength.
14. Hehre, W. J.; Radom, L.; Schleyer, P. v. R.; Pople, J. A. *Ab Initio Molecular Orbital Theory*; John Wiley & Sons: New York, NY, 1986.
15. Parr, R. G.; Yang, W. *Density Functional Theory of Atoms and Molecules*; Oxford University: New York, NY, 1989.
16. Becke, A. D. J. *Chem. Phys.* **1993**, *98*, 5648.
17. (a) Burke, K.; Perdew, J. P.; Wang, Y. In *Electronic Density Functional Theory: Recent Progress and New Directions*; Dobson, J. F., Vignale, G., Das, M. P., Eds.; Plenum: New York, NY, 1998; (b) Perdew, J. P. In *Electronic Structure of Solids '91*; Ziesche, P., Eschrig, H., Eds.; Akademie: Berlin, 1991; p 11; (c) Perdew, J. P.; Chevary, J. A.; Vosko, S. H.; Jackson, K. A.; Pederson, M. R.; Singh, D. J.; Fiolhais, C. *Phys. Rev. B* **1992**, *46*, 6671; (d) Perdew, J. P.; Chevary, J. A.; Vosko, S. H.; Jackson, K. A.; Pederson, M. R.; Singh, D. J.; Fiolhais, C. *Phys. Rev. B* **1993**, *48*, 4978; (e) Perdew, J. P.; Burke, K.; Wang, Y. *Phys. Rev. B* **1996**, *54*, 16533.
18. (b) Dunning, T. H., Jr.; Hay, P. J. In *Modern Theoretical Chemistry*; Schaefer, H. F., III, Ed.; Plenum: New York, NY, 1976; Vol. 3, p 1; (b) Hay, P. J.; Wadt, W. R. *J. Chem. Phys.* **1985**, *82*, 270; (c) Wadt, W. R.; Hay, P. J. *J. Chem. Phys.* **1985**, *82*, 284; (d) Hay, P. J.; Wadt, W. R. *J. Chem. Phys.* **1985**, *82*, 2299.
19. Ehlers, A. W.; Böhme, M.; Dapprich, S.; Gobbi, A.; Höllwarth, A.; Jonas, V.; Köhler, K. F.; Stegmann, R.; Veldkamp, A.; Frenking, G. *Chem. Phys. Lett.* **1993**, *208*, 111.
20. (a) Ditchfield, R.; Hehre, W. J.; Pople, J. A. *J. Chem. Phys.* **1971**, *54*, 724; (b) Hehre, W. J.; Ditchfield, R.; Pople, J. A. *J. Chem. Phys.* **1972**, *56*, 2257; (c) Hariharan, P. C.; Pople, J. A. *Mol. Phys.* **1974**, *27*, 209; (d) Gordon, M. S. *Chem. Phys. Lett.* **1980**, *76*, 163; (e) Hariharan, P. C.; Pople, J. A. *Theor. Chim. Acta* **1973**, *28*, 213.